Properties of Turbulent Flows

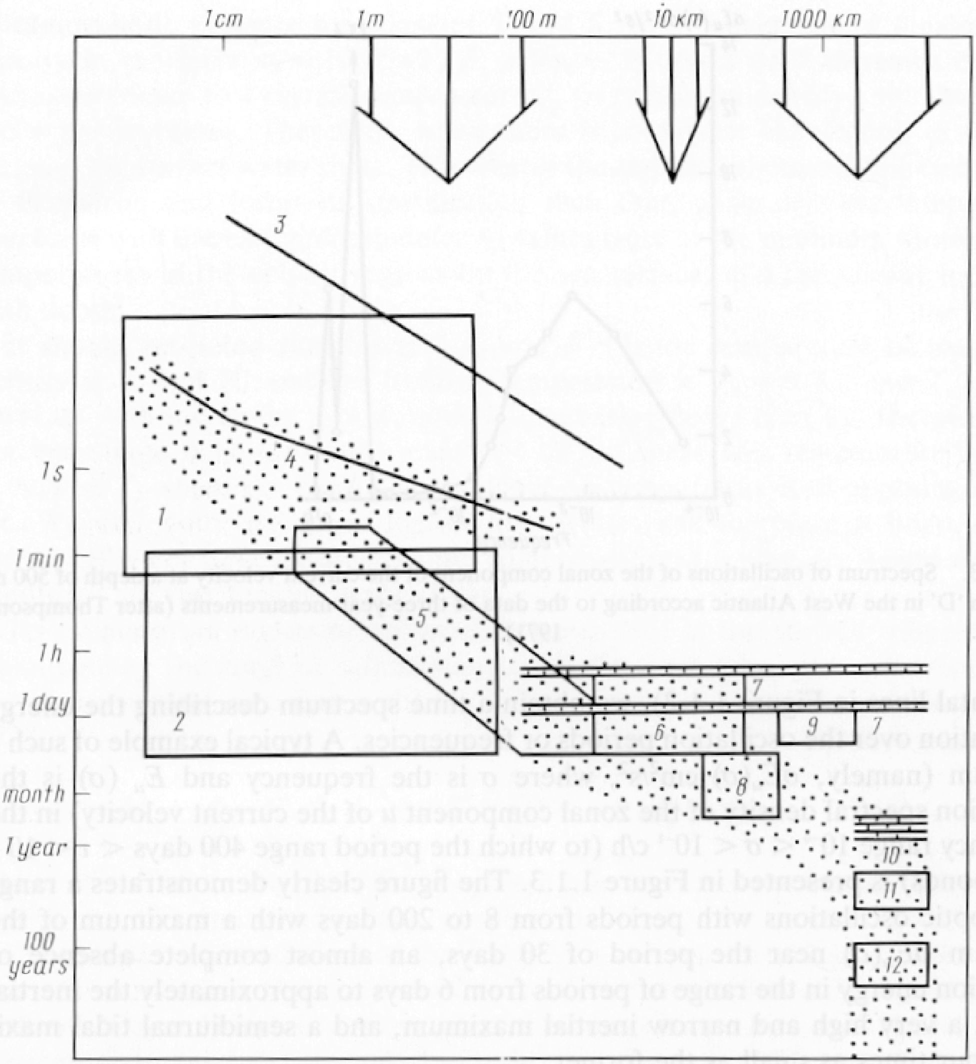

Fig. 1.1.2. Regions of spatial and temporal scales of various physical processes in the ocean. 1: small-scale turbulence; 2: vertical microstructure; 3: acoustic waves; 4: capillary and surface gravitational waves; 5: internal waves; 6: inertial oscillations; 7: tidal oscillations; 8: oceanic eddies and Rossby waves; 9: atmospheric synoptic processes; 10: seasonal variations; 11: major oceanic currents; 12: stratification of the ocean.

1 Smallest scales

It is often convenient to split the velocity field into two parts: $<\underline{u}>$ to represent the large–scale flow we wish to describe in detail and $\underline{u}'$ representing smaller scale fluctuating motions, or turbulence. Thus

$$\underline{u} = <\underline{u}> + \underline{u}'$$

where $<>$ represents some averaging process (time, space, ensemble).

Note that $<\underline{u}'> = 0$ and $<<\underline{u}> + \underline{u}'> = <\underline{u}>$.

We can split the tracer concentration, θ, in a similar manner:

$$\theta = <\theta> + \theta'$$

A measure of the strength of the turbulence is the turbulent kinetic energy defined as

$$q^2 = \frac{1}{2}(<u'^2> + <v'^2> + <w'^2>)$$

where u', etc. are the fluctuating components of the flow velocity in the three space dimensions (x, y, z). A measure of the fluctuations in concentration is the variance

$$<\theta'^2>$$

Turbulent fluctuations can only exist down to a finite scale. Molecular diffusion will eventually wipe out variations in the flow properties.

The smallest scale of the flow is given by the *Kolmogorov scale*

$$L_k = 2\pi \left(\frac{\nu^3}{\epsilon}\right)^{1/4}$$

which is determined on dimensional grounds assuming the kinematic viscosity, ν ($\sim$ O(10^{-6} m^{2}s^{-1}) for sea water), and the rate of turbulent kinetic energy dissipation, ϵ, are the only relevant quantities. ϵ is related to the turbulent K.E. by $\epsilon \simeq q^3/\mathcal{L}$, where $\mathcal{L}$ is a typical lengthscale of the turbulent flow (assuming the production of turbulent K.E. is balanced by dissipation). In the interior of the ocean $\epsilon \sim 10^{-9}$ W/kg (equivalent to the energy dissipated by one hair dryer per cubic kilometer of ocean). L_k is then about 4 cm. Close to the surface of the ocean which is being forced by the action of the wind $\epsilon \sim 10^{-7}$ W/kg or more (Brainerd and Gregg, 1995). L_k is then reduced to 1 cm or less.

The smallest scale for fluctuations of a tracer, such as temperature, is given by the *Batchelor scale*

$$L_b = 2\pi \left(\frac{D^2\nu}{\epsilon}\right)^{1/4}$$

where D is the molecular diffusivity of the tracer. For temperature $D_T \sim$ O(10^{-7} m^{2}s^{-1}) and, in the ocean interior, L_b is about 1cm. For salt $D_S \sim$ O(10^{-9} m^{2}s^{-1}) and L_b is about 1mm.

2 Turbulence

102. Instability of an axisymmetric jet. A laminar stream of air flows from a circular tube at Reynolds number 10,000 and is made visible by a smoke wire. The edge of the jet develops axisymmetric oscillations, rolls up into vortex rings, and then abruptly becomes turbulent. *Photograph by Robert Drubka and Hassan Nagib*

2.1 Shear Instability

Many environmental flows are unstable leading to the production of turbulence. As an example we consider Kelvin-Helmholtz instability. An inviscid stratified shear layer with an inflection point (i.e. $d^2U/dz^2 = 0$ some where in the flow) is unstable to Kelvin-Helmholtz instability if the stratification is sufficiently weak. For a parallel shear flow Miles (1960) showed that instability cannot occur if the Richardson number

$$Ri = N^2/(dU/dz)^2 > 1/4$$

where $N = -(g/\rho_o)\partial\rho/\partial z)$, the buoyancy frequency. For smaller values of Ri, instability usually does occur.

2.2 Turbulent Kinetic Energy Equation

Assuming vertical scales are much smaller than horizontal scales then the equation of the turbulent kinetic energy (TKE), q^2, becomes

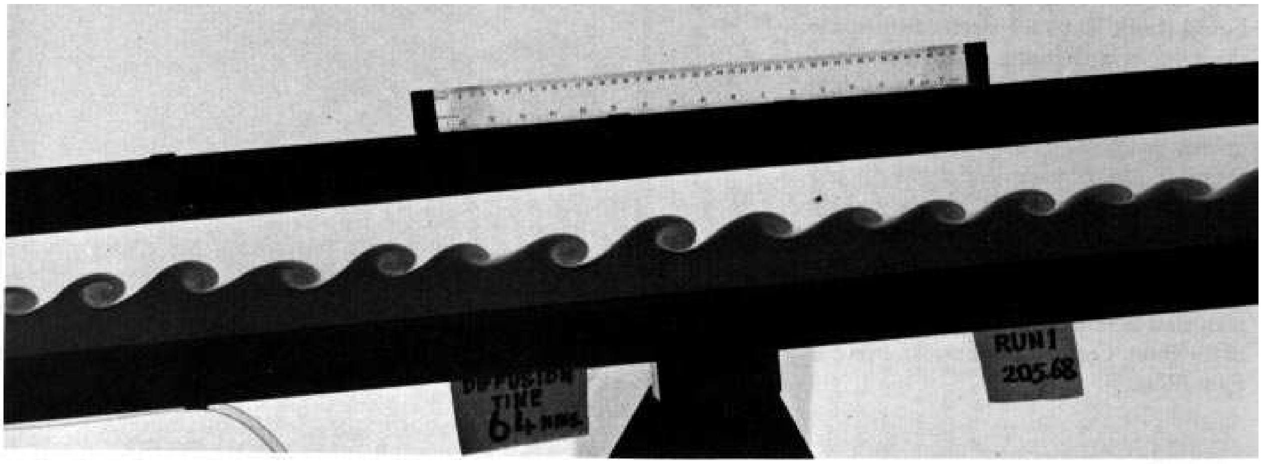

145. Kelvin-Helmholtz instability of stratified shear flow. A long rectangular tube, initially horizontal, is filled with water above colored brine. The fluids are allowed to diffuse for about an hour, and the tube then quickly tilted six degrees, setting the fluids into motion. The brine accelerates uniformly down the slope, while the water above similarly accelerates up the slope. Sinusoidal instability of the interface occurs after a few seconds, and has here grown nonlinearly into regular spiral rolls. *Thorpe 1971*

van Dyke, p. 85

$$\left(\frac{\partial}{\partial t} + \overline{\mathbf{u}} \cdot \nabla\right) q^2 = -\overline{u'w'}\frac{\partial \overline{u}}{\partial z} - -\overline{v'w'}\frac{\partial \overline{v}}{\partial z} + \overline{w'b'} - \frac{\partial}{\partial z}\left(\overline{w'q^2} + \frac{1}{\rho_0}\overline{w'p'}\right) - \nu\overline{\left[\left(\frac{\partial u}{\partial z}\right)^2 + \left(\frac{\partial v}{\partial z}\right)^2\right]}$$

Hence TKE is generated by (a) shear production

$$P = -\overline{u'w'}\frac{\partial \overline{u}}{\partial z} - -\overline{v'w'}\frac{\partial \overline{v}}{\partial z}$$

and (b) buoyant production

$$B = \overline{w'b'}$$

and lost through dissipation

$$\epsilon = \nu\overline{\left[\left(\frac{\partial u}{\partial z}\right)^2 + \left(\frac{\partial v}{\partial z}\right)^2\right]}$$

The remaining term

$$T = -\frac{\partial}{\partial z}\left(\overline{w'q^2} + \frac{1}{\rho_0}\overline{w'p'}\right)$$

(transport and pressure work) redistributes the TKE.

Shear production of TKE occurs if P is positive and represents a transfer of kinetic energy from the mean to the turbulent flow. The buoyant production term may be positive (generation of kinetic energy, loss of potential energy, as in convection) or negative (loss of KE, increase in PE, as in a stably stratified flow).

Both the production and dissipation of TKE are important elements of the turbulence. Without production the turbulence will be dissipated. The flux Richardson number

$$R_f = -B/P$$

characterizes whether the flow is stable or unstable. For values of R_f below some critical value $R_{f_{crit}}$ we expect the flow to be unstable. Estimates of the critical value suggest $R_{f_{crit}} = 0.15$

If the turbulence is stationary (i.e. D/Dt(TKE) = 0), and we integrate over a volume bounded by surfaces through which there are no energy fluxes, then there is a balance between production and dissipation of TKE, namely

$$P + B = \epsilon$$

Defining an eddy diffusivity for density, K_ρ, as $K_\rho = -B/N^2$ (assuming the flow is stably stratified) and using the above expression we can write K_ρ in terms of the flux Richardson number

$$K_\rho = \frac{R_f \epsilon}{(1 - R_f)N^2}$$

suggesting (Osborn, 1980)

$$K_\rho < 0.2 \frac{\epsilon}{N^2}$$

(note, the expression is often taken as an equality.)

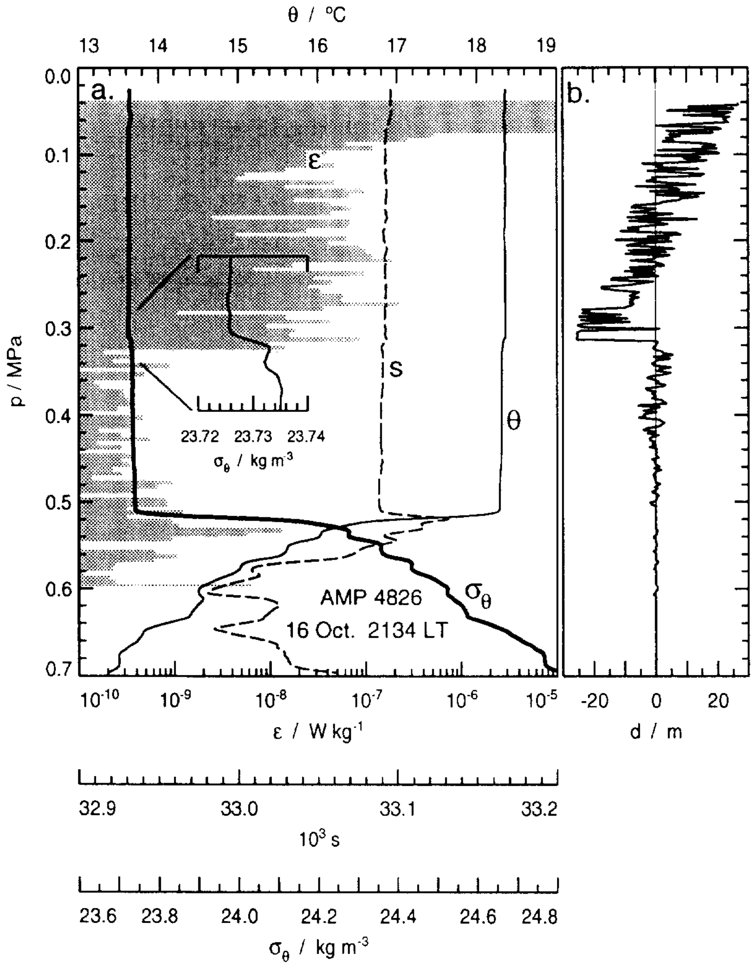

Fig. 1. Profile taken during convective deepening on PATCHEX: 2134 LT (local time, UTC—8 h). Panel a. Profiles of ϵ, θ, salinity and σ_θ. The shading is ϵ, estimated in 0.5 m bins; θ and σ_θ have been processed with a 0.8 m triangular filter. The small density step at 0.32 MPa (inset) is the bottom of the mixing layer. Panel b. Thorpe displacements; the large instability extending down to 0.31 MPa fills the active mixing layer.

from Brainerd and Gregg (1995)

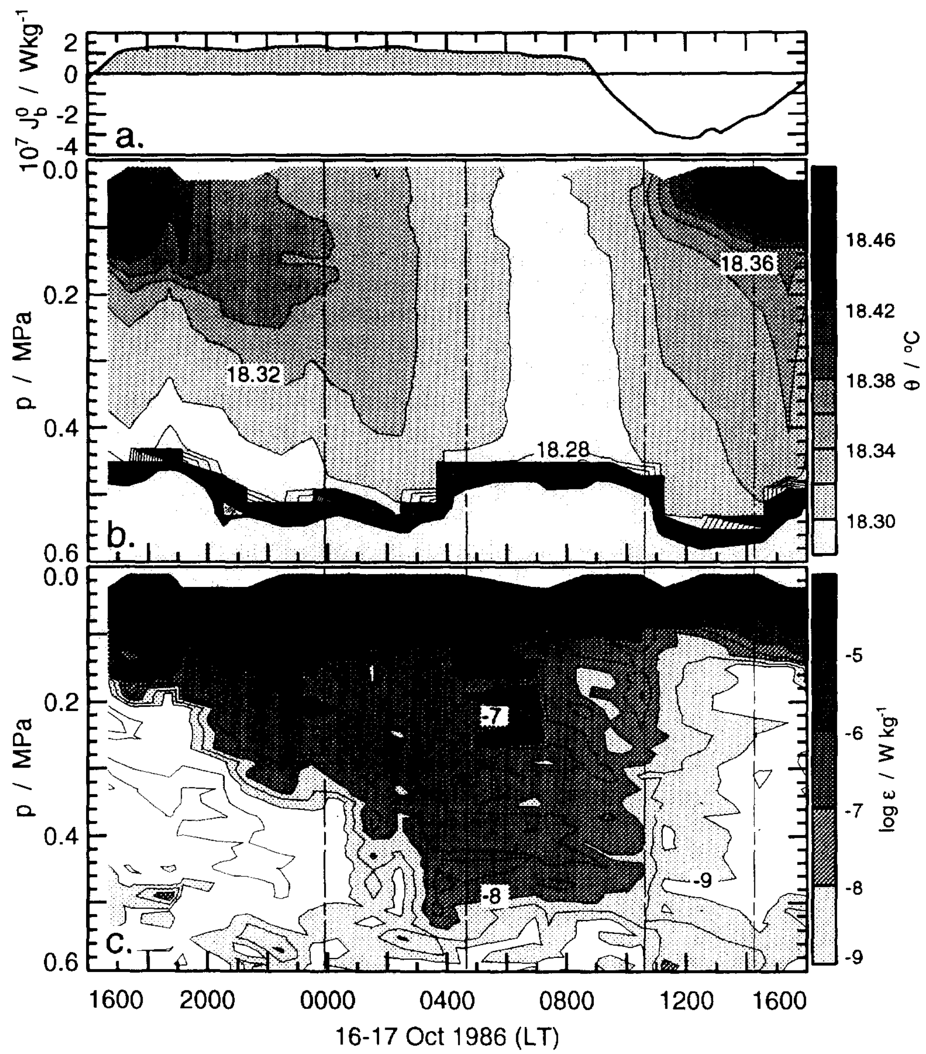

Fig. 6. A one-day cycle from PATCHEX. The vertical dashed lines mark the times of profiles shown in Fig. 7. Panel a. Surface buoyancy flux J_b^0. Panel b. Contours of θ, hour averages in 2 m vertical bins. Contour interval 0.02°C. Heavy black line is the top of the seasonal thermocline. Panel c. Contours of log ε: hour averages in 2 m vertical bins. Contour interval 0.5.

from Brainerd and Gregg (1995)

3 Spectra

3.1 3D turbulence

At smaller scales (e.g. within turbulent boundary layers) turbulence tends to be three dimensional. The effects of vortex stretching produces a cascade of kinetic energy from large to the smaller scales, ending at the Kolmogorov scale where turbulent kinetic energy is dissipated by viscosity. To see this we consider the domain averaged turbulent kinetic energy, $E =< \frac{1}{2}q^2 >$ and enstropy, $Z =< \frac{1}{2}|\underline{\omega}'|^2 >$, where $<>$ is now taken as a domain average, and $\underline{\omega}$ is the vorticity. Vortex stretching has a tendency to increase the enstrophy, Z, of the flow, whilst at scales somewhat larger than the Kolmogorov scale, L_k, the flow is essentially inviscid and the kinetic energy, E, is conserved. E and Z are related by

$$\frac{E}{Z} \sim \mathcal{L}^2$$

where $\mathcal{L}$ is the length scale of the most energetic eddies. If E is constant whilst Z increases, then $\mathcal{L}$ must decrease.

A statistically steady state can be achieved by forcing the turbulent flow at some large scale and dissipating energy at the Kolmogorov scale. Assuming there is an intermediate scale, known as the *inertial subrange*, where the flow is inviscid, we can determine the shape of the kinetic energy spectrum, $E(k)$, within this subrange, as a function of the wavenumber k, by a purely dimensional argument (Kolmogorov, 1941). The kinetic energy spectrum is the energy per unit mass per unit wavenumber and has dimensions

$$E(k) \sim L^3 T^{-2}$$

Within the inertial subrange the only thing which determines the flow of energy through wavenumber space is the rate at which it is being dissipated in the *viscous subrange*, ϵ. Therefore $E(k)$ can only depend on ϵ and k with

$$E(k) \sim \epsilon^m k^n$$

Since $\epsilon \sim L^2 T^{-3}$, we must have

$$E(k) \sim \epsilon^{\frac{2}{3}} k^{-\frac{5}{3}}$$

3.2 2D turbulence

At larger scales the effects of the Earth's rotation and stratification causes the flow to be predominantly two dimensional (the Taylor–Proudman theorem for a homogeneous fluid). For a stratified fluid the flow will be predominantly along isentropic/isopycnic surfaces. The effect of vortex stretching (a key ingredient of 3D turbulence) is much reduced and one can show that (in the absence of forcing or dissipation) the domain averaged enstrophy, Z, is now conserved. The consequence of this is that energy is cascaded to larger length scales (an *inverse* or *red* cascade) whilst enstropy cascades to smaller scales. (This is easily shown by considering the case of energy initially at a given wavenumber, k, being partitioned between wavenumbers $k/2$ and $2k$, and recalling that $Z(k) = k^2 E(k)$.)

Since the kinetic energy undergoes an inverse cascade there is little kinetic energy at small scales and hence dissipation. Enstropy on the other hand does cascade to smaller scales where it is dissipated. We can go through the same argument we did before to determine the spectral slope in an inertial subrange, but now considering enstrophy (rather than kinetic energy). Thus we expect

$$Z(k) \sim \frac{L}{T^2} \sim \epsilon_z^m k^n$$

where ϵ_z is the rate of enstrophy dissipation ($\sim 1/T^3$). Then

$$Z(k) \sim \epsilon_z k^{-1}$$

and

$$E(k) \sim \epsilon_z k^{-3}$$

At larger scales a second inertial range exists. The scaling for energy for 3D turbulence is equally valid for 2D turbulence, hence at larger scales

$$E(k) \sim k^{-5/3}$$

(see Kraichnan, 1967 for a fuller discussion)

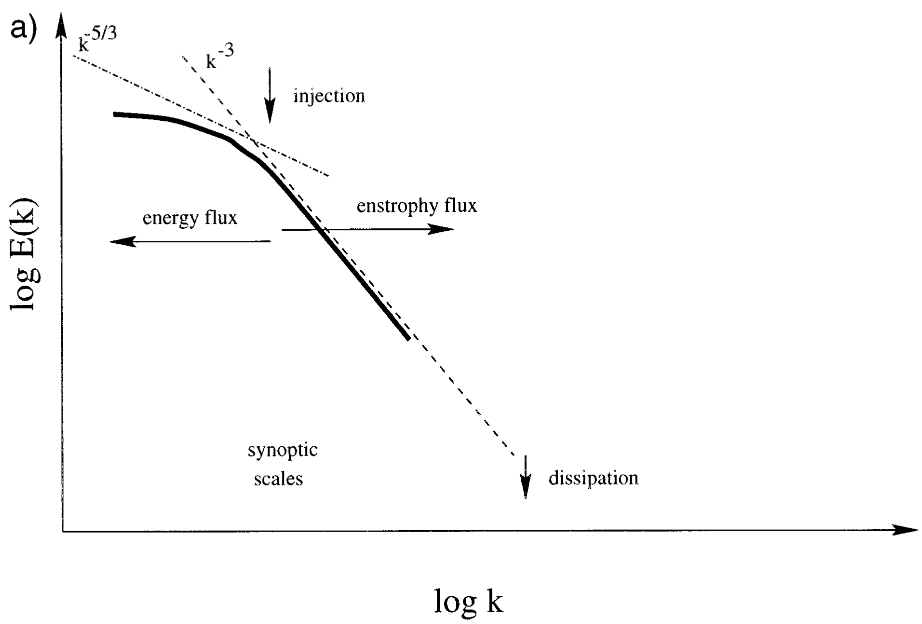

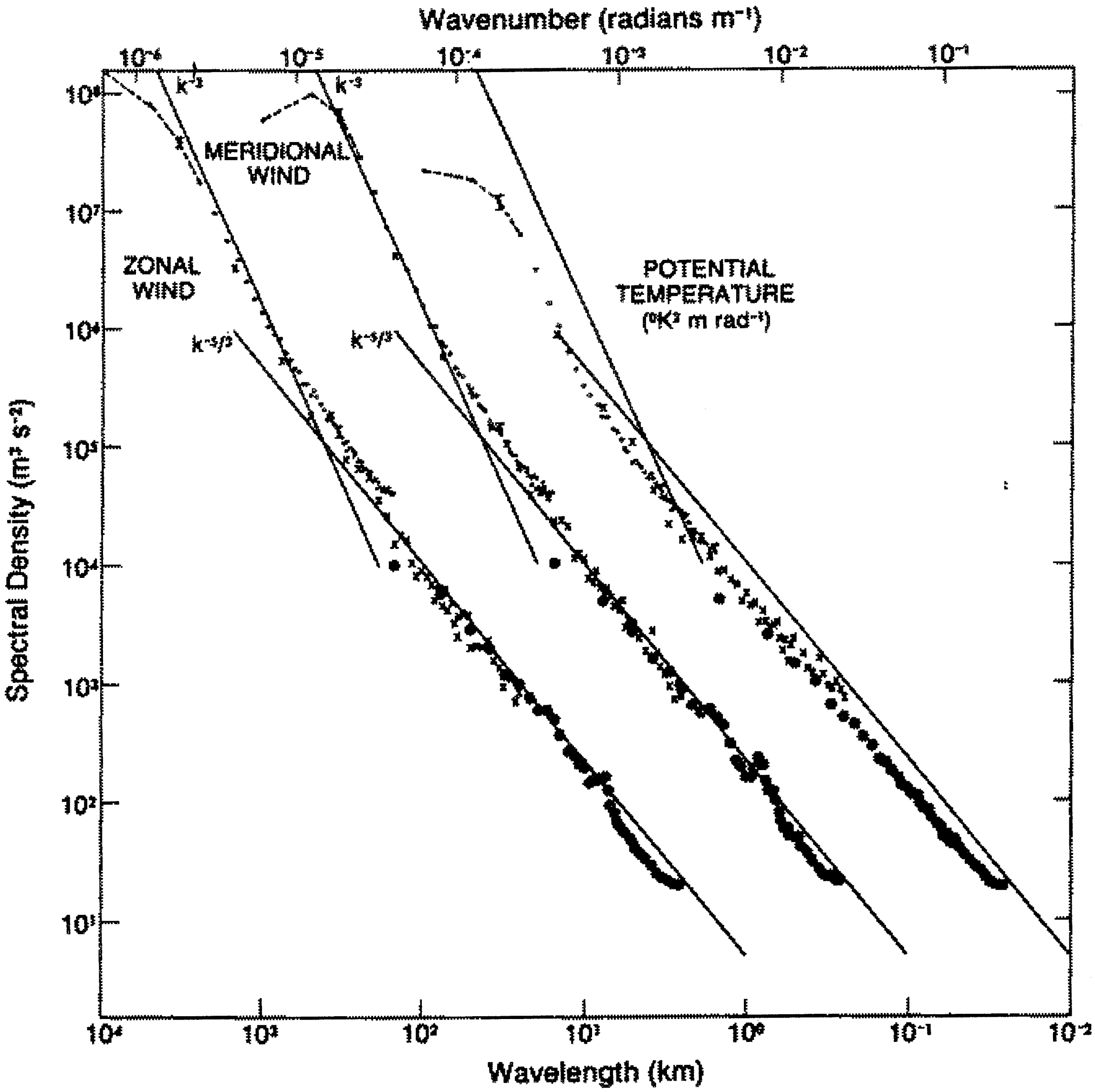

FIG. 1. Variance power spectra of wind and potential temperature near the tropopause from GASP aircraft data. The spectra for meridional wind and temperature are shifted one and two decades to the right, respectively; lines with slopes −3 and −5/3 are entered at the same relative coordinates for each variable for comparison. [Reproduced with permission from Nastrom and Gage (1985).]

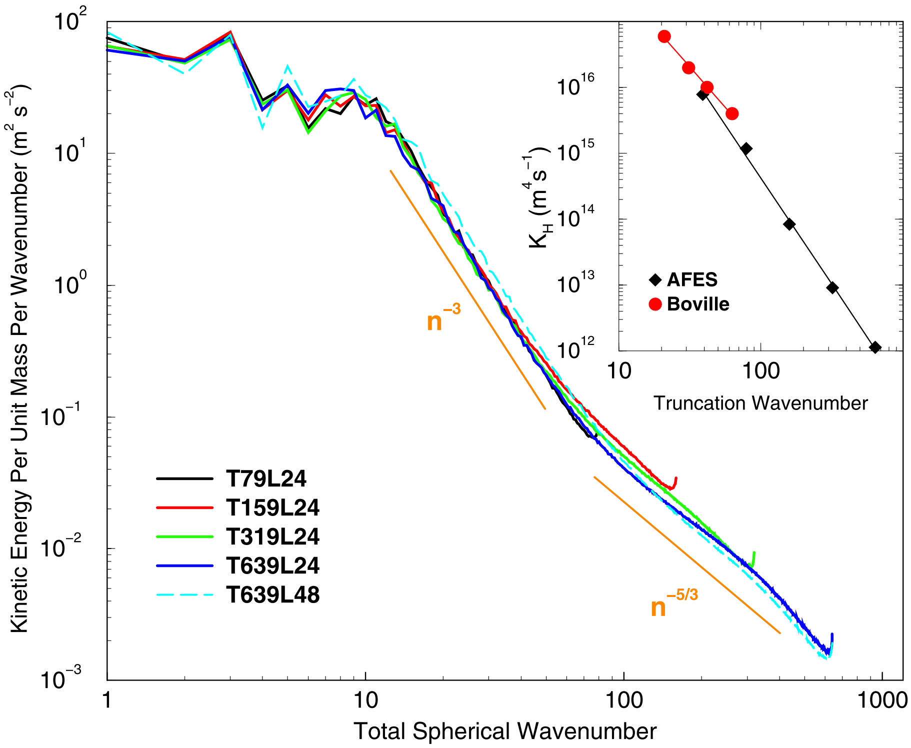

Figure 3. As in Figure 2 but for AFES run with different numerical resolution. Results are shown for the 24 level version truncated at T79, T159, T319 and T639, as well as the T639L48 version. At each horizontal resolution a diffusion coefficient has been determined by trial and error to produce the fairly convergent behavior at the high wavenumber end of the spectrum. The black symbols in the inset show the diffusion coefficient as a function of truncation obtained this way. The red dots show results from a similar analysis of a version of the NCAR atmospheric model obtained by *Boville* [1991]. The lines in the inset are linear regressions.

from Takahashi et al (2006)

Lindborg (2005) and Brethouwer *et al* (2007) have put forward a scaling argument for rotating stratified turbulence, backed up by numerical simulations, that give $E_k(k_h) \sim \epsilon^{2/3} k_h^{-5/3}$, and $E_k(k_v) \sim N^2 k_v^{-3}$.

3.3 Coherent structures

The spectral characteristics of the flow does not tell us everything. In particular, a feature of two–dimensional turbulence is the occurrence of long–lived intense vortices. The presence of these vortices has a profound effect on the dispersion of tracers in such a flow field by trapping the tracer for extended periods and acting as a *transport barrier*. We will consider the impact of the flow topology on tracer transport in a later lecture.

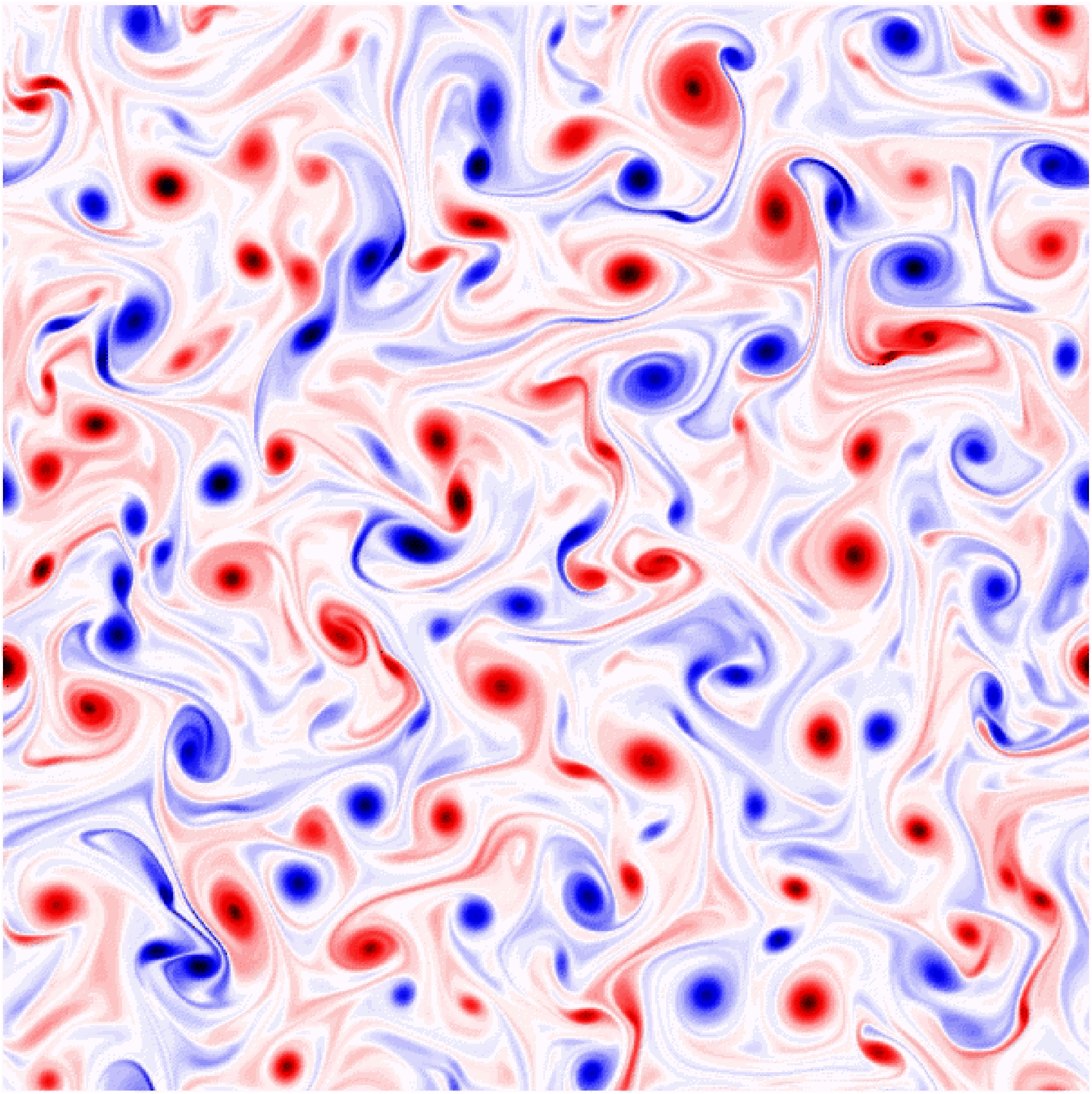

3.4 Halt to the inverse cascade

The inverse cascade is halted by something known as the β *effect*. At sufficiently large scales the flow is influenced by the variation in the Coriolis parameter, f, with latitude, namely $\beta = df/dy$, which acts as a restoring force. The scale at which this occurs is

$$L_\beta = \left(\frac{U}{\beta}\right)^{\frac{1}{2}}$$

called the *Rhines scale* (Rhines 1975), where U is a typical velocity scale. Above this scale the inverse energy cascade is inhibited. The following figures give examples of the flow that emerges

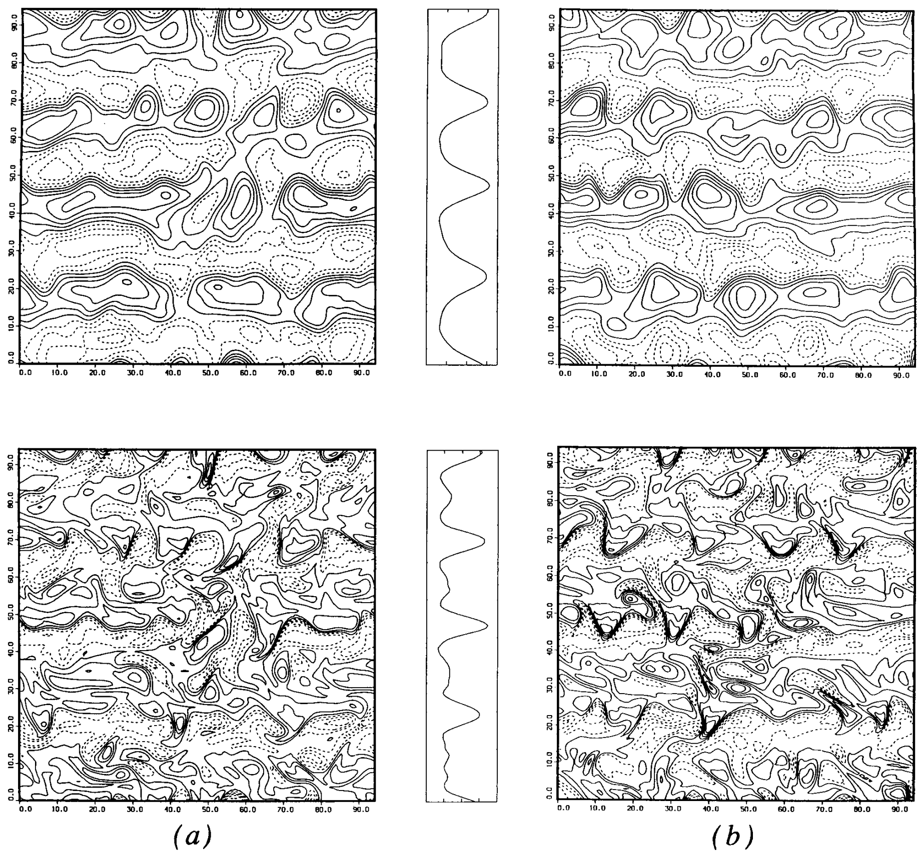

FIG. 7. Instantaneous fields (negative contours dashed). (a) Upper-layer eddy streamfunction (upper panel) and potential vorticity (lower panel) at time 2090 of the long integration. (b) Same as (a) but time 2100. Between the two panels are time averages (2000–3200) of zonally averaged zonal wind and meridional potential vorticity gradient; (c) and (d) show eddy barotropic (upper panel) and baroclinic (lower panel) at times 2090 and 2100, respectively. The contour intervals for baroclinic fields are ⅓ those of barotropic fields. (e) Instantaneous upper-layer eddy streamfunction fields taken from experiment with parameters as in Fig. 3a for times 625 (upper panel) and 700 (lower panel).
Pannetta (1993)

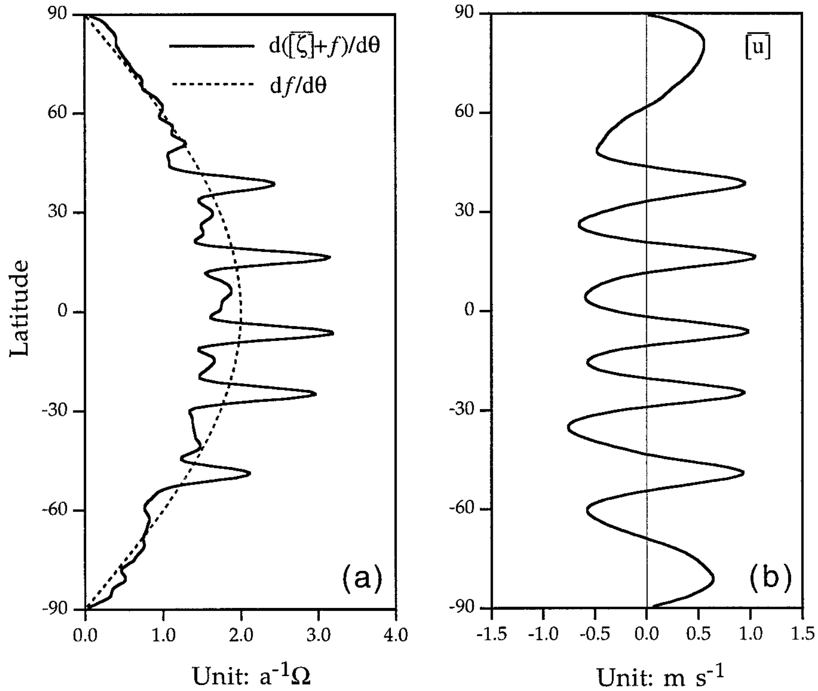

FIG. 9. (a) Time-mean meridional gradient of zonal-mean absolute vorticity (solid curve) and planetary vorticity (dashed curve) for case VIII. (b) Time-mean zonal wind profile (in m s^{-1}).

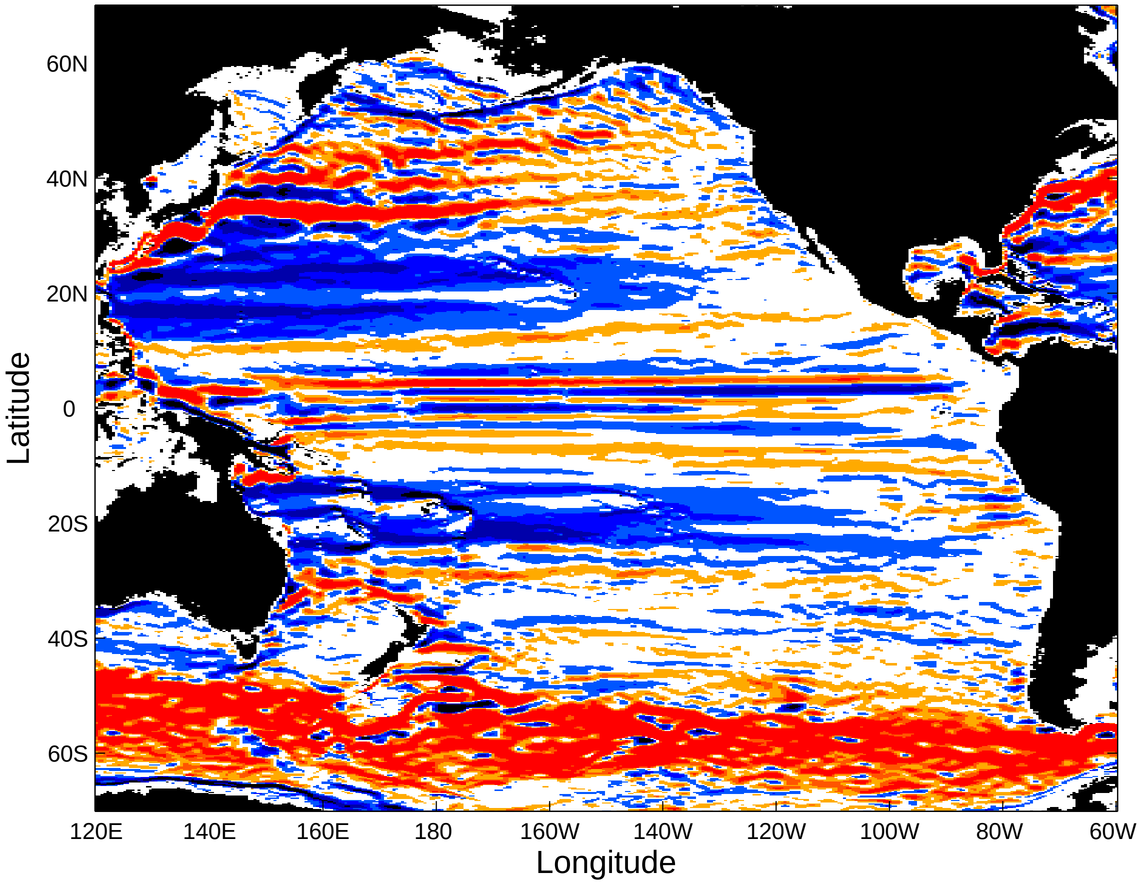

From Richards et al (2006), showing the multiple jet-like flow produced in a high resolution Ocean General Circulation Model (OFES).

References

Brainerd K.L., and M.C. Gregg, Surface mixed and mixing layer depths, *Deep Sea Research I*, *42*, 1521–1543, 1995.

Brethouwer G., P. Billant, E. Lindborg and J.-M. Chomaz, Scaling analysis and simulation of strongly stratified turbulent flows, *J. Fluid Mech.,* 585, 343–368.

Kolmogorov A., The local structure of turbulence in incompressible viscous fluid for very large Reynolds number (English translation 1991), *Proc. Roy. Soc. London A,* 434, 9–13, 1941a.

Kolmogorov A., Dissipation of energy in locally isotropic turbulence (English translation 1991), *Proc. Roy. Soc. London A,* 434, 15–17, 1941b.

Kraichnan R.H., Inertial ranges in two-dimensional turbulence, *Physics Fluids,* 10, 1417–1423, 1967.

Lilly D.K., Stratified turbulence in the atmospheric mesoscales, *Theoretical and Comp. Fluid Dyn.,* 11, 139–153, 1998.

Lindborg E., The effect of rotation on the mesoscale energy cascade in the free atmosphere, *Geophys. Res. Lett.,* 32, L101809.

Maltrud EM, and G.K. Vallis, Energy and enstrophy transfer in numerical simulations of two–dimensional turbulence, *Phys. Fluids A*, *5*, 1760–75, 1993.

Miles J.W., The hydrodynamic stability of a thin film of liquid in uniform shearing motion, *J. Fluid Mech.*, *8*, 593–610, 1960.

Nastrom G.D., and K.S. Gage, A climatology of atmospheric wavenumber spectra of wind and temperature observed by commercial aircraft, *J. Atmos. Sci.,* 42, 950–960, 1985.

Osborn, T.R., Estimates of the local rate of vertical diffusion from dissipation measurements, *J. Phys. Oceanogr.,* 10, 83–89, 1980.

Pannetta R.L., Zonal jets in wide baroclinically unstable regions: persistence and scale selection, *J. Atmos. Sci.*, *50*, 2073–2106.

Phillips O.M., The Komogorov spectrum and its oceanic cousins: a review, *Proc. Roy. Soc. London A,* 434, 125–138, 1991.

Provenzale A., Transport by coherent barotropic vortices, *Annual Rev. Fluid Mech.,* 31, 55–93, 1999.

Rhines P.B., Waves and turbulence on a beta-plane. *J. Fluid Mech.,* 69, 417–443, 1975.

Rhines P.B., Geostrophic turbulence. *Annual Rev. Fluid Mech.,* 11, 401–441, 1979.

Richards, K. J., N. A. Maximenko, F. O. Bryan, and H. Sasaki, Zonal jets in the Pacific Ocean, *Geophys. Res. Lett.,* 33, L03605, doi:10.1029/2005GL024645, 2006.

Sinha B., and K.J. Richards, Jet structure and scaling in Southern Ocean models, *J. Phys. Ocean.,* 29, 1143–1155.

Takahashi Y. O., K. Hamilton and W. Ohfuchi, Explicit global simulation of the mesoscale spectrum of atmospheric motions, *Geophys. Res. Lett.,* 33, L12812, doi:10.1029/2006GL026429, 2006.